Constraints on the Neogene – Quaternary Geodynamics of the Southern Urals: Comparative Study of Neotectonic Data and Results of Strength and Strain Modeling Along the URSEIS Profile

Valentine O. Mikhailov[1], Arcady V. Tevelev[2]., Robert G. Berzin[3], Elena A. Kiseleva[1], Ekaterina I. Smolyaninova[1], Arsen K. Suleimanov[3], Elena P. Timoshkina[1]

[1] United Institute of Physics of the Earth, RAS, Moscow, Russia

[2] Moscow State University, Moscow Russia

[3] "Spetsgeofizika", Moscow, Russia

Corresponding author: Valentine O. Mikhailov

E-mail: mikh@uipe-ras.scgis.ru

tel. 7 (095) 254 8577, FAX: 7 (095) 254 6040

Much geological and geomorphologic evidence indicates that the modern topography of the Southern Urals has been formed during the Neogene – Quaternary due to superposition of, (1) NW-SE compression and asymmetric uplift of the area as a whole, and (2) more vigorous transpressive uplift of the Central and Western Uralian blocks in the Late Pliocene – Quaternary. Strength modeling based on data on the deep structure, temperature and composition of the crust revealed that the Western and Central Uralian blocks are characterized by low total strength. Numerical strain modeling showed that vertical Neogene -Quaternary movements of the area can be a consequence of intraplate compression, maximum deformation being concentrated in weak blocks. The model predicts different deformational style in the upper and lower parts of inhomogeneous Uralide crust: the zone of maximum deformation at the top of the crust occurs in the Main Uralian fault zone while, in the lower crust, it is shifted 70 km to the west, where a vertical Moho offset (the so-called Makarovo fault) is located. Thus, this fault could have developed (or at least been sufficiently renewed) during Neogene -Quaternary.

1. INTRODUCTION

Much new data have been recently acquired for the Southern Urals, especially along the URSEIS profile [*Berzin et al.,* 1996; *Carbonell et al*., 1996; *Echtler et al*., 1996*; Knapp et al.,* 1996; *Brown et al*., 1997; *Juhlin et al*., 1997; *Poupinet et al*., 1997; *Diaconescu et al*., 1998; *Steer et al.,* 1998; *Tevelev et al*., 1998]. In addition to models on the deep structure [e.g., *Berzin et al.*, 1996; *Carbonell et al*., 1996; *Echtler et al*., 1996; *Knapp et al.*, 1996] new thermal [*Kukkonen et al*., 1997] and gravity [*Döring et al*., 1997] models as well as new fission track data [*Seward et al*., 1997, 2002] have been published. These data allow a better understanding of the present structure and evolution of the Southern Urals. Nevertheless, some results obtained by different geological and geophysical methods seem to contradict each other. This relates, for example, to data on the age of modern topography and Neogene - Quaternary geodynamics of the Southern Urals.

Much evidence points to the conclusion that the Urals topography is comparatively young [e.g., *Trifonov*, 1960; *Lider*, 1976; *Borisevich,* 1992; *Stephanovsky et al.*, 1997; *Puchkov,* 1997; *Tevelev et al*., 1998]. Based on different geologic and geomorphologic data, these authors suggested that Urals topography has been developed during the Neogene-Quaternary. On the other hand, recent preliminary fission-track results obtained for the west-east transect of the Southern Urals [*Seward et al*., 1997] showed zircon and apatite fission-track ages about 200 Ma and more. A number of investigators explained these data as evidence that the present-day topography of the Southern Urals is a remnant of relief resulting from Paleozoic deformation [e.g. *Diaconescu and Knapp*, 2002]. On the other hand, additional study of zircon and apatite fission track ages led *Seward et al.* [2002] to the conclusion that the present relief of the Ural mountains is likely a product of a post-Uralide events and not of the Uralide orogeny itself.

The goal of the present paper is to study the mechanism and temporal development of the modern relief of the Southern Urals. To do this we considered geological and geomorphologic data and correlated them to data on the structure and lithospheric strength of different tectonic zones in the vicinity of the URSEIS profile. We demonstrated that uplifts occurred in blocks characterized by lower present-day strength. Using results of strength calculations we carried out numerical modeling of deformation of the southern Uralide lithosphere. For it we employed a simple mechanical model, which simulates the main structural features of the Southern Urals along the URSEIS profile. This modeling showed that topography similar to the modern topography of the Southern Urals can result from horizontal compression of the model by far-field forces alone. Thus, using neotectonic data on Neogene-Quaternary uplift of the region it appears possible to obtain a self-consistent model of modern structure and geodynamics of the Southern Urals.

2. NEOTECTONIC MOVEMENTS IN THE SOUTHERN URALS

The main topographic features of the Southern Urals and the location of the URSEIS profile are presented in Figure 1. Many researchers of the geology of the Uralides [*Trifonov*, 1960; *Schults*, 1969; *Lider*, 1976; *Borisevich,* 1992; *Puchkov,* 1997; *Stefanovsky,* 1997] have considered the Southern Urals to have been tectonically active during the Cenozoic. *Schults* [1969] for the first time compared the Southern Urals with such active and well-known regions as Tien-Shan, and found clear similarities in their neotectonic development. According to *Lider* [1976], rapid uplift of the Urals took place at the beginning of the Quaternary, when several hundred meters of coarse gravel was accumulated on the western margin of the West Siberia Depression. These Early Mindel sediments are recognized as molasse of Early Pleistocene orogeny. At the Likhvin time (Mindel - Riss) the lower edge of the East Uralian plateau could be

two or three times higher than at present. During the Middle Pleistocene and, in particular, Late Pleistocene, neotectonic movements were strongly inhomogeneous [*Borisevich,* 1992; *Tevelev, et al.,* 1998]. Relatively uplifted areas were cut by series of flat erosional surfaces, correlated with alluvial terraces of the main rivers of the Urals. The actual ages of these geomorphologic complexes in the vicinity of the URSEIS profile was for a long time in dispute, because they were inferred only from morphological and lithological correlations [*Tevelev, et al.,* 2002]. Our dating based on floral remnants confirmed the Quaternary age of these complexes. Thus, in general, the current relief of the Southern Urals is more likely newly formed than inherited. Published evaluations on the amplitude and rate of Quaternary uplift in the region are diverse. We consider the estimates given by *Trifonov* [1960] as the most reliable. Based on repeated geodetic measurements he estimated the rate of uplift of the Southern Urals at the latitude of the town of Miass to be 0.45 cm/year and the total Quaternary uplift to be about 1 km [see also, *Borisevich,* 1992].

Evidence of recent tectonic activity in the Southern Urals is found in the western periphery of the region, nearly at the western end of the URSEIS profile. Here, in the Belaya-river valley there is a zone of sedimentation similar to that of a foredeep, which started to develop in front of the Southern Urals during the Late Miocene [*Shilts,* 1969]. The coal-bearing Miocene sediments are folded, and it seems probable that the evolution of the main features of the modern topography started with these deformation events. The Pliocene – Quaternary sediments in this depression seem to be composed of both proximal and distal components. The latter are represented almost exclusively by of series of Caspian transgressions [*Tevelev et al.,* 2002]. The well-studied Apsheron (early Quaternary) and Akchagyl (pre-Quaternary) transgressions definitely reached this zone, but spatial configuration of the corresponding basins has not

coincided with modern valleys of the Belaya, Ural and Volga rivers. This suggests a young age for these river valleys, which have probably been developed during the Pleistocene when relief in the area was finally re-shaped.

In fact, there are no data supporting the existence of Late Jurassic relief in the region. According to *Puchkov* [1997] since the end of the Jurassic and during the Cretaceous the Urals were a lowland partly covered by a sea. In the Early Cretaceous, and in part of the Late Cretaceous, a sea strait between the Polar Urals and the Mediterranean sea basins occupied the area of the Ufimian plateau situated to the north of the Southern Urals; thus, no subaerial relief existed here. In the Late Cretaceous, a wide sea basin occupied the eastern margin of the East European platform. It included the boundary zone of the Urals, and in the Paleogene (at least in the Paleocene) the orientation of sea basins did not coincide with the strike of the Uralides. Thus, the Uralides probably did not control a geomorphologic structure of the region at that time. The eastern slope of the South Urals is in general exhumed from beneath Eocene sediments and has also Neogene to Quaternary geomorphologic age.

Interpretation of known geological and geomorphologic data [*Sigov,* 1969; *Borisevich,* 1992; *Tevelev et al.,* 1998; *Makarova et al.,* 2000; *Tevelev et al.,* 2002] allow us to suggest that deformation of the Southern Urals in the Neogene-Quaternary time has been complex. Deformation evolved under oblique (NW-SE) compression and consisted, (1) of regional asymmetric arch-shaped uplift, involving the whole area from the Kopeysk fault zone on the east to the Shikhan fault zone on the west (with the maximum uplift being on the order of several hundreds meters), and (2) of more vigorous (of order of thousand meters) superimposed transpressive uplift of the Central Uralian and Western Uralian zones, pushed up along weak marginal zones inherited from old strike-slip faults. Left-lateral transpression, uplift and

development of mountain structures in this region correlates with the main stage of Alpine orogeny in surrounding orogens [*Shults,* 1969; *Tevelev and Tevelev,* 1996; *Tevelev et al.,* 1998]. Thus, most likely the Ural mountains represent a part of the collisional collage caused by the India-Eurasia interaction. Deformation started at the end of the Oligocene, was especially active in the Late Pliocene – Late Quaternary time, and is still active now. Deformation is manifest in structure-dependent distribution of the Late Pleistocene - Holocene subsiding and elevated areas on the East Uralian Plateau [*Tevelev et al.,* 1998, *Tevelev et al.,* 2002, see also Figure 1b], as well as in data of geodetic and horizontal stress measurements [*Puchkov,* 1997; *Zubkov and Lipin,* 1997].

Based on this deformational model we estimated a rate of vertical neotectonic movement along the URSEIS profile. We used a standard procedure of comparing present-day topographic height of pre-orogenic geomorphologic surfaces (see Figure 1a) with the proposed height of their formation. The most reliable estimates can be obtained for the eastern and western ends of the profile, situated within (or next to) the areas of Oligocene to Miocene marine shallow water sedimentation. We suppose that sea level in these basins was close to the modern one, so the present-day altitude of the basins is close to the post-Miocene elevation. In the central part of the profile (in the regions of the East Uralian Plateau, Central and Western Uralian Uplifts) altitudinal position of the pre-orogenic surface is inferred from analysis of spatial and temporal relations between continental flat erosional surfaces of the Pliocene to Late Pleistocene age. We took into consideration the general curvature of these surfaces, and amplitude of sequential erosional cuttings, interactions with Cenozoic depositional complexes.

At the eastern termination of the URSEIS profile, Oligocene marine sediments, which are about 20 – 30 meters thick, are now situated at a height of 230 – 250 meters. Thus, a reasonable

value of uplift here for the Neogene – Quaternary is 250-300m. Amplitude of uplift increases smoothly up to 500m at the western boundary of the Zingeika block, where the altitude of the flat erosional surface exhumed from beneath the Paleogene deposits reaches up to 450 m.

To the west, in the Magnitogorsk block, recent relief has developed over very thick island arc complexes. Amplitudes of the Neogene-Quaternary uplift vary from 400-450 m near the east margin of the Magnitogorsk block (Gumbeika river valley) where continental deposits of pre-Neogenean age are situated at an altitude of 350 – 400 m, to 800m near the Main Uralian Fault, in the vicinity of which the Early Cenozoic complexes are denuded and the altitude of the Pliocene topographic surfaces is about 600-700 m. The Main Uralian fault separates the Magnitogorsk block from the Central transpressive block; the latter includes the Central Uralian and Western Uralian uplifts. Relief within the block is completely erosional; the denudation of pre-deformational surface is roughly estimated at 200 m, so maximum elevation of the Central Uralian uplift along the profile is about 1300 m, and elevation of the Western Uralian uplifts is 1200-1000 m from east to west. The western boundary of the block is also represented by a set of strike-slip and reverse faults, and marked by systems of surficial scarps and young sedimentary deposits. The structural pattern of the neotectonic units suggests that deformation of the Central Uralian uplift was governed by diagonal nearly NW-SE compression, which is consistent with instrumental present-day stress measurements [*Zubkov and Lipin,* 1997].

The western end of the profile crosses the Urals foredeep, which is partly involved in the recent uplift of the region. Total vertical deformation there consists of a regional component (uplift of the Southern Urals as a whole) and local subsidence during the recent activity. Minimum amplitudes (150-200m in accumulated topography) are in the Belaya River area. The amplitude

of uplift increases to the west up to 400-450 m, toward the East European platform marginal anticline structures.

The latest results of zircon and apatite fission-track analysis [*Seward et al.,* 2002] support the young age of Uralian relief. According to these authors disturbance of the apatite age-altitude relationship shows that the Uralian mountains are the result not of the Uralide orogeny, but of reactivation of old structures that determines distribution of present-day weak zones.

3. STRENGTH OF THE LITHOSPHERE ALONG URSEIS PROFILE

To estimate the strength of the Uralide lithosphere we calculated yield strength profiles using data on the structure, temperature and composition of the lithosphere in the vicinity of the URSEIS profile. We first consider the geothermal data.

Heat flow in the Uralides has been determined from several hundred measurements of temperature and thermal parameters of rocks taken from deep boreholes. The most complete catalogue of heat flow data was collected by *Golovanova* [1994]. The characteristic features of heat flow in the Southern Urals are as follows.

Heat flow in the eastern part of the Eastern European platform ranges between 35-45 mW/m^2. Nearly the same heat flow values are found at the western slope of the Urals. In the Magnitogorsk block the heat flow values are considerably lower – about 25 mW/m^2. The zone of comparatively low values is relatively narrow but it stretches for at least 1500 km from 48^o N to 60^o N. To the east of the Magnitogorsk block heat flow increases to more than 40 mW/m^2. The heat flow decrease in the Magnitogorsk block can be attributed to a number of factors including: (a) high permeability of the rocks, which permit heat transfer from uplifted areas to surrounding foredeeps by underground waters; (b) paleoclimate; (c) low heat generation in rocks of the Magnitogorsk block; (d) low heat flow from the mantle below the Central Urals. Detailed

analysis of the possible contribution of each of these factors led *Kukkonen et al.* [1997] to the conclusion that the main factor responsible for the heat flow minimum is low heat generation in rocks of the Magnitogorsk block.

It is worth noting that the distribution of temperature in the upper lithosphere does not differ substantially in different thermal models [*Bulashevich and Shapov,* 1983; *Salnikov,* 1984; *Khutorskoy,* 1985; *Kukkonen et al.,* 1997; *Khachay and Druzhinin,* 1998], as all the models have the same heat flow and temperature at the Earth surface. Thus, estimates of the strength of the upper lithosphere should be similar. We used the model of lithosphere structure, composition, and temperature distribution suggested by *Kukkonen et al.* [1997]. This very detailed thermal model was suggested for the Troitsk DSS profile situated close to the URSEIS one and crossed the same tectonic units. We used this model to characterize relative variation of the strength of the lithosphere in the main blocks of the Southern Urals. The model of the deep structure used by *Kukkonen et al.* [1997] was slightly modified in the Magnitogorsk block to be closer to data of URSEIS profile (Figure 2a).

To estimate mechanical properties of lithospheric rocks we calculated yield strength profiles using the conventional approach [*Ranalli and Murphy,* 1987; *Kohlstedt et al.,* 1995; *Evans and Kohlstedt,* 1995]

$$\sigma = \min\{\alpha \cdot \rho \cdot g \cdot z(1-\lambda);\ (\dot{\varepsilon}/A_d)^{1/n} \cdot \exp(E/n \cdot R \cdot T)\}, \qquad (1)$$

where $\sigma = \sigma_{\max} - \sigma_{\min}$ is the difference between maximum and minimum principal stresses, α is a coefficient depending upon the type of fault ($\alpha = 3.0$, 1.2 and 0.75 for thrust, transcurrent and normal faulting [*Ranalli, 1997*]); $\rho \cdot g \cdot z$ is the overburden pressure (product of density, gravitational acceleration and depth); λ is the ratio of fluid pore pressure to lithostatic pressure; $\dot{\varepsilon}$ is a strain rate; A_d and n are the Dorn constants, studied by laboratory experiments for

different types of rocks; E is an activation energy; R is the universal gas constant; T is the rock temperature (K^o).

Strength diagrams calculated for eight different tectonic units crossed by the URSEIS profile are presented in Figure 3 (location of these units is shown in Figure 2a). It is worth noting that creep parameters have been measured for a limited number of different rock types. As a result, it is difficult to find a close analog for every petrologic unit found in outcrops and boreholes or suggested for deep layers of the Southern Urals. Diagrams presented in Figure 3 were calculated using creep parameters of marble and quartzite as strength characteristics for the rocks marked by number 1 on Figure 2a; granite and quartz-diorite data for the layers 2,3, and 4; anorthosite and quartz-diorite data for the layers 5 and 6; and olivine data for the layers marked 7 and 8. As usual, when a layer consists of several rock types, the minimum yield strength value was adopted for the strength profile. It appeared that for the thermal conditions of the Southern Urals, yield strength of the upper layer (marked 1 and 2) was mainly determined by brittle failure and only in its lower part (diagrams II, IV, VI) by the power low creep of quartzite, so changes of composition of this layer can not change the strength diagrams. Strength of the layers from 2 to 6 was controlled by brittle failure or power law creep of quartz-diorite. Thus, even though in strength calculations we used many rock types, the final strength profiles were determined by only three: quartzite, quartz-diorite and olivine. Their creep parameters are given in Table 1. The similar strength distribution was obtained replacing quartz-diorite by mafic granulite (Table 1). When replacing olivine rheology in layer 7 by the rheology of dry peridotite (Table 1), the relative distribution of the total strength along profile remains the same, even the strength of layer 7 reduces considerably above the Moho discontinuity. Thus, stress estimates and especially

estimates of the total strength appeared to be stable with regard to variations of rock composition.

The coefficient $\alpha(1-\lambda)$ was assigned a value of 2, averaging α values for the thrust and transcurrent faulting, and also taking into account the possible influence of the pore pressure (when pressure is hydrostatic coefficient λ is equal to 0.38 [*Kohlstedt et al.,* 1995]). Strain rate was assumed to be equal to $\dot{\varepsilon} = 10^{-16}\ c^{-1}$. This value was obtained from numerical modeling of neotectonic movements, which yields maximum $\dot{\varepsilon}$ for the Neogene -Quaternary in the range 4 - 6 $10^{-16}\ c^{-1}$ (see section 4.2 and Figure 4 for more details).

There are two main brittle layers on the strength diagrams for the Southern Urals (Figure 3). The first one is a brittle layer in the upper crust (which can be subdivided into two sub-layers as on diagrams II, IV, VI) and the second one is a brittle layer incorporating an area above the Moho and continuing into the upper mantle. The existence of the brittle layer above and below the Moho indicates that faults traced on seismic profiles can disrupt the Moho discontinuity (Makarovo fault, for example, see *Diaconescu et al.* [1998]). It is also important to note that not all of the profiles contain the brittle layer below the Moho (see diagrams III, IV, VI). Absence of brittle layers in the middle crust indicates that faults in the upper crust should not extend directly to deeper parts of the crust.

An important characteristic of lithospheric blocks appears to be total strength, which is the result of integration of the strength profiles over depth. The highest total strength has been obtained for the Eastern European platform ($9.3 \cdot 10^4$ *MPa·km*), the Western Siberian basin ($9.0 \cdot 10^4$ *MPa·km*), and the Zingeika block ($8.6 \cdot 10^4$ *MPa·km*). Moderate values of total strength have been found for the Plast ($7.3 \cdot 10^4$ *MPa·km*) and the Trans-Uralian blocks ($7.5 \cdot 10^4$ *MPa·km*). Relatively low total strength is found for the Western Uralian and Central Uralian uplifts ($6.4 \cdot 10^4$

MPa·km) as well as the Urals foredeep ($6.7 \cdot 10^4$ *MPa·km*) and the Magnitogorsk block ($7.0 \cdot 10^4$ *MPa·km*). These results are in good agreement with the location of zones of maximum deformation and high rates of neotectonic movements: maximum deformation has occurred in the zones of low total strength.

4. NUMERICAL MODELING

4.1 *Background*

In this section we consider the results of numerical modeling of deformation for a simple mechanical model simulating the main features of the Southern Urals structure along the URSEIS profile.

For modeling of slow, long-term (several My) deformation at the neotectonic stage, we used a simple 2D model of a viscous Newtonian medium. It is possible to use more sophisticated models, although any model will only be a rough approximation of the very complicated structure that is the lithosphere, the Southern Uralide lithosphere in particular. The style of deformation in the simple model described below mainly depends on the non-homogeneous distribution of mechanical properties. Similar styles of deformation can be obtained using other models, in particular the pure elastic one (see below).

In our model the lithosphere comprises three layers: the upper "rigid" 5-km thick layer having apparent viscosity 10^{24} *Pa·s*, the "ductile" (having low horizontally inhomogeneous viscosity) 35-km thick layer and a "rigid" 10-km thick layer having apparent viscosity 10^{24} *Pa·s* situated above and below the Moho (see the diagrams in Figure 3). Horizontal inhomogeneity of the crust was simulated by variations of effective viscosity of the middle "ductile" layer over two orders of magnitude (Figure 2b). Based on strength estimations the smallest effective viscosity value was assigned to the middle crust below the Central and Western Uralian uplifts: 10^{22} *Pa·s*; a

higher value of 10^{23} *Pa·s* was prescribed for the Urals foredeep; the value $5 \cdot 10^{23}$ *Pa·s* was used for the Magnitogorsk block. Other blocks had the same apparent viscosity values as the viscosity of the upper and the lower "rigid" layers, i.e. 10^{24} *Pa·s*.

The boundaries between the Urals foredeep and the Western Uralian uplift as well as between the Central Uralian uplift and the Magnitogorsk block (Figure 2b) were assumed dipping to the east [*Tryggvason et al.*, 2001]. The boundary between the Magnitogorsk and Trans-Uralian blocks was inferred to dip to the west. The density distribution along the profile was given in accordance with *Döring et al.* [1997]. It is necessary to point out that in the majority of tectonically active areas (including the Southern Urals, as will be shown in our calculations), regional deformation is driven almost exclusively by externally imposed intraplate forces [e.g., *Zoback,* 1992]), so local density variations do not strongly influence the results of the modeling.

Using the rheological law of Newtonian viscosity, the velocity field within the model is determined by solving the Stokes equations. We assumed material incompressibility and an absence of body forces other than those of gravity. The upper boundary is assumed to be stress free.

The processes that have produced the present-day topography of the Southern Urals are not completely understood. Topography might be caused by horizontal compression by far-field forces and by processes in the mantle below the Urals (e.g. convection, phase transitions). Thus, we have decided not to assign any boundary conditions based on existing geodynamical hypotheses, but to find them by solving the following inverse problem: to find the velocity fields on the side boundaries and at the base of the model so that the top of the model moves in accordance with the rates of neotectonic movements discussed previously. We used a similar

approach to estimate the state of stress in different regions [*Kolpakov et al*, 1991; *Smolyaninova et al*., 1996; *Stephenson and Smolyaninova,* 1999].

The problem of independently finding all components of the velocity vector (in the 2D case they are the horizontal *U* and the vertical *W* components) has no unique solution. It is clear, for example, from the fact that any distribution of the vertical component of the velocity vector at the top of the model can be obtained as a result of pure vertical movements at the base of the model with horizontal component equal to zero. To avoid this problem we link horizontal and vertical components of the velocity vector at the two vertical side boundaries and the base of the model by the equation:

$$W(x,z) = -(z - z_0)\,\partial U(x)/\partial x \qquad (2),$$

where x and z are horizontal and upward vertical coordinates respectively and z_o is a constant. This equation has been extensively used in sedimentary basin modeling (for references see *Cloetingh et al.* [1995]). This equation is based on the following assumption put forward by *Braun and Beaumont* [1989]: when the lithosphere is extended (or compressed) by intraplate forces, there is a horizontal level z_o which stays horizontal during the process of deformation in the absence of gravity. The same equation was obtained by [*Myasnikov and Savushkin,* 1978] in their consideration of the interaction of the lithosphere, asthenosphere and upper mantle. Using a model based on Newtonian viscosity they found that for regional structures which formed during time periods of several My and more, z_o coincides with the so-called free mantle or floating level. By definition, free mantle or floating level, z_{fm}, is an equilibrium level to which an inviscid mantle substratum could rise in a well crossing through the crust to the depth of the mantle. An equation relating z_o to the distribution of rheological properties of the lithosphere

assuming a linear relationship of stress and strain (i.e., for an inhomogeneous effective elastic plate) was obtained by *Mikhailov* [1999].

When z_o does not coincide with the free mantle level, intraplate extension or compression disturbs local isostatic equilibrium. For small deformations of a thin plate this disturbance (referred to as a load) can be found from the equation [e.g., *Mikhailov,* 1999]:

$$q(x) = -(z_0 - z_{fm})\,\partial U/\partial x\,/(1 + \partial U/\partial x)\,. \qquad (3)$$

Corresponding vertical isostatic movements can be found using the model of a thin elastic plate [*Braun and Beaumont,* 1989]. In this paper we assigned $z_0 = z_{fm}$, neglecting the role of flexural rigidity of the rocks in the process of the Urals foredeep formation, as shortening and deformation in the Urals foredeep in Neogene - Quaternary were small, especially in comparison to the Paleozoic ones [*Brown et al*., 1997].

Thus, we have solved the inverse problem to find $W_0(x)$, the vertical component of the velocity vector at the base of the model, under the condition that it provides a best fit to the rates obtained from the geomorphologic data. To solve this problem numerically, the function $W_0(x)$ was presented as an expansion in a series of elementary functions. The number of functions in this expansion should be less than the number of points where neotectonic data are assigned. Strictly speaking, this inverse problem is unstable; one of the possible ways to arrive to a stable solution is by the reduction of the number of elementary functions. Using the finite element method [e.g., *Zienkevich and Taylor,* 1989] the problem of deformation of the viscous medium was solved for every elementary function of the unit amplitude. After that, amplitude of all the elementary functions was found under the condition of the mean square deviation of calculated vertical component of the velocity vector at the top of the model and geomorphologic data. For a Newtonian medium this problem is linear (see *Smolyaninova et al*. [1996] for more details). For

the present case the length of the profile was supposed to be 504 km, depth of the model was 50 km, and the size of mesh was 73x19 (horizontal x vertical).

It should be stressed that the bottom boundary of the model need not coincide with any physically interpretable boundary because the horizontal component of the velocity vector in the lithosphere below the bottom of the model is supposed to be independent of *z* (see equation (2)). The only point is that it has to be deeper than the main structural inhomogeneities affecting the stress field, while the ratio of horizontal to vertical dimensions of the model must be much greater than unity (as, strictly speaking, equation (2) is valid only for the thin-sheet model). For more details, see *Stephenson and Smolyaninova* [1999].

When the boundary conditions are determined, components of the stress tensor within the model and other parameters characterizing the deformation of rocks can be calculated [e.g., *Smolyaninova et al.,* 1996]. In our study we used the octahedral shear stress and the ratio of the octahedral shear stress to the mean pressure (so-called damage parameter). This parameter can be used to characterize deformation by rock failure or frictional sliding. In areas where this parameter is large, development of faults or movement along pre-existing faults is more likely [*Byerlee,* 1968].

4.2 *Results of Numerical Modeling*

Results of the inverse problem solution are shown in Figures 4 to 6. Figure 4a demonstrates the quality of the inversion: both the calculated and observed curves of the vertical movements at the surface of the model are very similar. Calculated vertical and horizontal components of the velocity vector at the base of the model are shown in Figure 4 b, c.

The horizontal component of the velocity vector at the base of the model (Figure 4c) looks very simple. It is nearly constant near the left and right sides of the model where deformation is

small and has two almost linear intervals which coincide with areas of compression in weak zones of the model. Such a distribution corresponds to simple intraplate compression of the model by forces applied at its side boundaries. Thus, no tectonic forces acting at the bottom of the model are necessary to explain neotectonic movements of the Uralides. Generally, the obtained solution may have been much more complicated. For example, to explain rather complex neotectonic movements along the profile Crimea-Black Sea [*Smolyaninova et. al,* 1996], it appeared necessary to include some mantle-induced movements at the bottom of the model.

It can be seen from Figures 4a and 4b that the compression is localized mostly in areas which correspond to the Western and Central Uralian uplifts. Considerably less deformation took place in the Magnitogorsk block and the Urals foredeep. An important peculiarity of the velocity distribution is an offset of the maximum of the vertical velocity at the base of the model in relation to its maximum at the surface. At the surface of the model (Figure 4a) the maximum of the vertical velocity is between 280 and 310 km (i.e. in the Central Uralian uplift area), while at the bottom of the model (Figure 4b) the vertical velocity reaches maximum between 380 and 350 km, which corresponds to the Western Uralian uplift. Absolute values of the vertical velocity at the surface and at the Moho are comparatively small. If the magnitude of the velocities in the Southern Urals region are of the same order, then the total vertical displacement over the last 10 My would be about several kilometers. Taking into account the low thermal gradient with depth (Figure 2), which appears not to have changed considerably during the last 10 My, one can conclude that these movements were not able to exhume rocks from depths of 15-20 km corresponding to the 300° isotherm. Thus, fission track data do not contradict the suggestion that present-day topography has been formed during the Neogene – Quaternary.

Horizontal offset of the area of maximum deformation at the top of the model in relation to its bottom is well demonstrated by Figure 5, where the distribution of the horizontal component of velocity is shown by isolines. Arrows show the direction of movement, their length corresponds to absolute values of the velocity vector in relation to the left side of the model. To make variations of the vertical component of velocity in Figure 5 visible, the scale for the vertical component was set 10 times greater than for the horizontal one.

It can be seen from Figure 5 that the "rigid" plate at the top of the crust and the other one near the Moho deform in different ways. The area of maximum horizontal shortening (where the vertical component of the velocity vector reaches the maximum value) in the upper layer is offset 70 km eastward in comparison to the area of maximum horizontal shortening of the lower "rigid" layer. This offset is a result of the geometry of the low viscosity zone in the middle part of the model (Figure 2b). When side boundaries of the low viscosity zone are vertical there is no horizontal offset of zones of maximum horizontal shortening in the upper and lower layers. This offset was accompanied by detachment of the lower plate in relation to the upper one along the low viscosity zone in the middle crust in the central part of the model.

Distribution of the octahedral shear stress is presented on Figure 6a. As boundary conditions of the mechanical problem were not boundary forces, but components of the velocity vector (neotectonic movements at the top as well as horizontal components of velocity vector at the bottom and the side boundaries), the relative distribution of stress does not depend on the absolute values of the viscosity. The absolute values of stress are linearly proportional to the viscosity. If apparent viscosity of the lithosphere in both "rigid" layers is equal to 10^{24} $Pa\ s$, then stress units in the Figure 6b are MPa. Figure 6a demonstrates that the model, in general, is characterized by low values of the octahedral shear stress. There are two zones of maximum

values which coincide with “rigid” (according to diagrams on Figure 3, brittle) layers. The first one is at the surface of the model, embracing the area of the eastern part of the Uralian foredeep and the Western and Central Uralian uplifts. Faulting with thrusting of rigid blocks from east to west can develop there. The second zone of maximum shear stress is situated at the base of the crust below the Western Uralian and western part of the Central Uralian uplifts. Brittle deformation can also take place in this zone (diagram III in Figure 3) because it is characterized by high values of the damage parameter (Figure 6b). This zone coincides with the so-called Makarovo fault [e.g., *Diaconescu et al.,* 1998], an apparent 5 km vertical offset of the Moho discontinuity. Thus, this fault could have formed (or at least sufficiently rejuvenated) in the Neogene - Quaternary, contemporaneously with the formation of the modern topography. A distinctive feature of the Makarovo fault is that it has no analog in the upper crustal layers above it, which implies that this fault has a very old age [*Diaconescu et al.,* 1998]. Another possible explanation is based on the strength profiles and the octahedral shear stress distribution. They demonstrate that faults at the base of the crust can not extend to the surface because in the middle crust brittle failure should be replaced by ductile behavior. The slow flow pattern (Figures 5 and 6) shows that shortening of the lower rigid plate between 350 and 380 km is accommodated by shortening of the upper rigid plate not immediately above this zone, but at 70 km to the east in the Main Uralian Fault zone.

There are two other zones of high damage parameter values. The first one is between 170-120 km, which corresponds to the Suhteli blanket, a thrust zone which is characterized mostly by horizontal displacements (see arrows in Figure 6). The second one is under the Urals foredeep where multiple reflectors are observed in the middle of the crust [*Berzin et al*., 1996; *Tryggvason*

et al., 2001]. The direction of velocity vectors shows that displacements here should be nearly horizontal and small.

5. CONCLUSIONS

1. Geological and geomorphologic data suggest that the present topography of the Southern Urals has been formed during the Neogene-Quaternary. We consider complex deformation of the Southern Urals in this period being due to a superposition of, (a) diagonal NW-SE compression and asymmetric uplift of the Southern Urals area as a whole with maximum uplift of several hundreds meters, and (b) more vigorous superimposed transpressive uplift of the Central and Western Uralian blocks in the Late Pliocene – Quaternary of about one thousand meters.

2. Modeling of lithospheric strength along the URSEIS profile revealed highest crustal strength in the Western Siberian basin, the East European platform, and the Zingeika block. Moderate strength values were obtained for the Plast and Trans-Uralian blocks. The strength of the crust below the Urals foredeep and the Magnitogorsk block, and especially below the Western and Central Uralian uplifts, is considerably lower (25% less). This is in a good agreement with the location of the zones of maximum deformation and rates of neotectonic movement in the Southern Urals.

3. We considered the deformation of a simple model of the lithosphere that includes the main features of the structure of the Southern Urals. It appeared from solution of the inverse problem with the use of geomorphologic data that movements at the Southern Urals during the Neogene – Quaternary can be governed by intraplate compression. The model predicts horizontal offset of the zones of maximum deformation at the top and the base of the crust. The maximum deformation near the surface took place in the area corresponding to the Central Uralian block while in the lower crust maximum deformation was offset to the west and occurred below the

area corresponding to the Western Uralian block. This area coincides with an offset in depth of the Moho discontinuity (the Makarovo fault). Thus, this fault could have developed or rejuvenated at the neotectonic stage of the Southern Urals formation.

Acknowledgement

We thank Alexander A. Savelyev (deceased), who attracted our attention to numerical modeling of neotectonic movements of the Southern Urals. We are grateful to two anonymous reviewers for very carefully reading the manuscript, constructive reviews and numerous suggestions, and language corrections. We also thank Robert Simpson (USGS) for language corrections. Attention and help of Dennis Brown, the volume editor, is greatly acknowledged.

REFERENCES

Berzin, R., O. Oncken, J. H. Knapp, A. Pérez-Estaún, T. Hismatulin, N. Yunusov, and A. Lipilin, Orogenic evolution of the Uralian mountains: results from an integrated seismic experiment, *Science*, *274*, 220-221. 1996.

Byerlee, J.D., Brittle-ductile transition in rocks, *J. Geophys. Res., 73*, 4741-4750, 1968.

Borisevich, D.V., Neotectonics of the Urals, *Geotectonics, 26,* 41-47, 1992.

Braun, J., and C. Beaumont, A physical explanation of the relationship between flank uplifts and the breakup unconformity at rifted continental margins, *Geology*, *17,* 760-764, 1989.

Brown, D., J. Alvarez-Marrón, A. Pérez-Estaún, Y. Gorozhanina, V. Baryshev, and V. Puchkov, Geometric and kinematic evolution of the foreland thrust and fold belt in the Southern Urals, *Tectonics, 16,* 551-562, 1997.

Bulashevich, Yu. P., and V.A. Schapov, Geothermal characteristics of the Urals, in *Application of geothermal data to regional study and geological prospecting,* (in Russian), edited by Yu. V. Bulashevich, B.P. Dyakonov, and Yu.V. Khachay, Acad. Sci. USSR, Uralian branch, Sverdlovsk, 3-17, 1983 (in Russian).

Carbonell, R., A. Pérez-Estaún, J. Gallart, J. Diaz, S. Kashubin, J. Mechie, R. Stadtlander, A. Schulze, J.H. Knapp, and A. Morozov, Crustal root beneath the Urals: wide-angle seismic evidence, *Science, 274,* 222-224, 1996.

Cloetingh, S., J.D. van Wees, P.A. van der Beek, and G. Spadini, Role of pre-rift rheology in kinematics of extensional basin formation: constraints from thermomechanical models of Mediterranean and intracratonic basins, *Mar. and Petrol. Geol., 12,* 793-807, 1995.

Diaconescu, C., J. H. Knapp, L. D. Brown, D. N. Steer, and M. Stiller, Precambrian Moho offset and tectonic stability of the East European platform from the URSEIS deep seismic profile, *Geology, 26,* 211-214, 1998.

Diaconescu, C.C., and J.H. Knapp, Role of a phase-change Moho in stabilization and preservation of the Southern Uralian orogen, Russia, in *Orogenic Processes in the Paleozoic Uralides,* edited by D. Brown, C. Juhlin, and V. Puchkov, AGU Geophys. Mon. Series, 2002 (this issue).

Döring, J., H-J. Götze, and M.K. Kaban, Preliminary study of the gravity field of the Southern Urals along the URSEIS'95 seismic profile, *Tectonophysics, 276*, 49-62, 1997.

Echtler, H.P., M. Stiller, F. Steinhoff, C. Krawczyk, A. Suleimanov, V. Spiridonov, J.H. Knapp, Y. Menshikov, J. Alvarez-Marrón, and N. Yunusov, Preserved collisional crustal structure of the Southern Urals revealed by vibroseis profiling, *Science, 274*, 224-226, 1996.

Evans, B., and D.L. Kohlstedt, Rheology of rocks, in *Rock physics and phase relations. A handbook of physical constants.* AGU Reference Shelf, *3,* 148-165, 1995.

Golovanova, I. V., *Catalog of the Uralian heat flow data* (in Russian), Russian Acad. Sci., Ufa Scientific Center, 1994.

Juhlin, C., M. Bliznetsov, L. Pevzner, T. Hismatulin, A. Rybalka, and A. Glushkov, Seismic imaging of reflectors in the SG4 borehole, Middle Urals, Russia, *Tectonophysics, 276,* 1-18, 1997.

Khachay, Yu.V. and V.S. Druzhinin, Geothermal cross-section of the Uralian lithosphere along latitudinal DSS profiles, *Izvestiya, Phys. Solid Earth, 34,* 59-62, 1998.

Khutorskoy, M.D., Heat flux and a model of structure and evolution of the lithosphere in the South Urals and Central Kazakhstan, *Geotectonics, 19,* 215-223, 1985.

Kirby, S.H. and A.K. Kronenberg, Correction to Rheology of the lithosphere: selected topics, *Rev. of Geophys., 25*, 1680-1681, 1987.

Knapp, J.H., D.N. Steer, L.D. Brown, R. Berzin, A. Suleimanov, M. Stiller, E. Lüschen, D.L. Brown, R. Bulgakov, S.N. Kashubin, and A.V. Rybalka, Lithosphere-scale seismic image of the Southern Urals from explosion-source reflection profiling, *Science, 274,* 2226-228, 1996.

Kohlstedt, D.L., B. Evans, and S.J. Mackwell, Strength of the lithosphere: Constraints imposed by laboratory experiments, *J. Geophys. Res. 100,* 17, 587-17, 602, 1995.

Kolpakov, N.I., V.A. Lyakhovsky, M.V. Mints, E.I. Smolyaninova, and Ye. Ye. Shenkman, Geodynamic nature of relief-forming processes on the Kola Peninsula, *Geotectonics*, *25*, 161-166, 1991.

Kukkonen, I. T., I.V. Golovanova, Yu.V. Khachay, V.S. Druzhinin, A.M. Kasarev, and V.A. Schapov, Low geothermal heat flow of the Urals fold belt – implication of low heat production, fluid circulation or paleoclimate? *Tectonophysics, 276*, 63-85, 1997.

Lider, V.A., *Quaternary deposits of the Urals* (in Russian), Moscow, Nedra, 1976.

Makarova, N.V., N.I. Korchuganova, and V.I. Makarov, Morphological types of orogens as indicators of geodynamical settings of their formation, *Geomorphology, 1,* 14 –28, 2000.

Mikhailov, V.O., Modeling of extension and compression of the lithosphere by intraplate forces, *Izvestya, Physics of the Solid Earth*, *35*, 228-238, 1999.

Myasnikov, V.P. and V.D. Savushkin, Small parameter method in the hydrodynamic model of the Earth's evolution, *Trans. (Doklady) Russian Acad. Sci./Earth Sc. Sec.*, *238,* 1083-1086, 1978.

Poupinet, G., F. Thouvenot, E.E. Zolotov, Ph. Matte, A.V. Egorkin, and V.A. Rackitov, Teleseismic tomography across the middle Urals: lithospheric trace of an ancient continental collision, *Tectonophysics, 276,* 19-33, 1997.

Puchkov, V.N., Structure and geodynamics of the Uralian orogen, in *Orogeny through time*, edited by J-B. Burg and M. Ford, Geol. Soc. London, Spec. Publ. 121, 201-236, 1997.

Ranalli, G., and D.C. Murphy, Rheological stratification of the lithosphere, *Tectonophysics, 132,* 281-295, 1987.

Ranalli, G., Rheology of the lithosphere in space and time, in: *Orogeny through time*, edited by J-B. Burg and M. Ford, Geol. Soc. London, Spec. Publ. 121,19-37, 1997.

Salnikov, V.E*., Geothermal regime of the Southern Urals* (in Russian), Moscow, Nauka, 1984.

Seward, D., A. Pérez-Estaún, and V. Puchkov, Preliminary fission-track results from the southern Urals – Sterlitamak to Magnitogorsk, *Tectonophysics, 276*, 281 –290, 1997.

Seward, D., D. Brown, R. Hetzel, M. Friberg, A. Gerdes, G.A. Petrov, and A. Perez-Estaut, The syn- and post-orogenic low temperature events of the Southern and Middle Uralides: evidence from fission-track analysis, in *Orogenic Processes in the Paleozoic Uralides,* edited by D. Brown, C. Juhlin, and V. Puchkov, AGU Geophys. Mon. Series, 2002 (this issue).

Schults, S.S., On the newest tectonics of the Urals (in Russian), in: *Materials on Geomorphology and Neotectonics of the Urals and the Volga Basin,* edited by V.P. Sigov, Ufa, 45 – 59, 1969,.

Sigov, A.P., *Metallogeny of the Mezozoic and Cenozoic deposits of the Urals* (in Russian), Moscow, Nedra, 1969, 296 pp.

Smolyaninova, E.I., V.O. Mikhailov, and V.A. Lyakhovsky, Numerical modeling of regional neotectonic movements in the Northern Black Sea, *Tectonophysics*, *266*, 221-231, 1996.

Steer, D.N., J.H. Knapp, L.D. Brown, H. P. Echtler, D.L. Brown, and R. Berzin, Deep structure of the continental lithosphere in an extended orogen: An explosive-source seismic reflection profile in the Urals (Urals Seismic Experiment and Integrated Studies (URSEIS 1995)), *Tectonics, 17,* 143-157, 1998.

Stefanovsky, V.V., Stratigraphy scheme of the quaternary deposits of the Urals (in Russian), in *Materials to stratigraphic scheme of the Urals (Mz,Kz),* edited by V.V. Stefanovsky, Ekaterinburgh, 93-139, 1997.

Stephenson, R.A., and E.I. Smolyaninova, Neotectonics and seismicity in the south eastern Beaufort Sea, polar continental margin of the north-western Canada, *Geodynamics, 27*, 175-190, 1999.

Tevelev, Al.V., Arc.V. Tevelev, I.A. Kosheleva, and E.F. Burstein, *Explanations to Geological Map of Russian Federation at the 1:200,000 scale. The South Uralian series* (in Russian), *Sheet N-41-XIX*, S-Petersburg, 2002.

Tevelev, Arc. V., and Al. V. Tevelev, Modern pull-apart basins of passive continental regions, in *Abstracts of the Lomonosov conference*, Moscow State University, 27-28, 1996.

Tevelev, Arc. V., and Al. V. Tevelev, Mode of recent evolution of the Eastern Urals, *6th Zonenshain conference on plate tectonics and Europrobe workshop on Uralides. Abstracts*. Moscow, Geomar, 203-204, 1998.

Trifinov, V.P., Main features of the Uralian neotectonics, in *Geomorphology and modern tectonics of Volga-Urals and Southern Urals regions* (in Russian), edited by V.V. Stefanovsky, Ufa, 293-300, 1960.

Tryggvason, A., D. Brown, and A. Pérez-Estaún, Crustal architecture of the southern Uralides from true amplitude processing of the URSEIS vibroseis profile, *Tectonics*, 2001, (in press).

Zienkiewicz, O.C., and R.L. Taylor, *The Finite Element Method*, 4th Ed., McGraw-Hill, New York, 1989.

Zoback, M.L., First and second order patterns of stress in the lithosphere: The world stress map project, *J. Geophys. Res., 97,* 11, 703-11, 728, 1992.

Zubkov, A.V., and Ya. J. Lipin, Stressed state of the Uralian uppermost crust, *Trans. (Doklady) of Russian Acad. Sci. 336*, 792 – 793, 1997

R. G. Berzin and A. K. Suleimanov, "Spetsgeofizika", Povarovka, Moscow District, Russia

E. A. Kiseleva, V. O. Mikhailov, E. I. Smolyaninova and E. P. Timoshkina, United Institute of Physics of the Earth, Russian Academy of Sciences, B. Gruzinskaya, 10, Moscow, 123810, Russia

A. V. Tevelev, Moscow State University, Geological Faculty, Vorobievy Gory, Moscow, Russia

Figure 1. Geomorphologic scheme of the Southern Urals.

a. topography along the URSEIS profile (meters vs. kilometers).

b. geomorphologic sketch map of the Southern Urals: 1- maximally uplifted blocks and massifs of the Central Uralian uplift; 2- comparatively high uplifted blocks and massifs; 3- blocks and massifs characterized by medium uplift; 4-boundaries of the modern orogen; 5-boundaries of structural geomorphologic units of the Southern Urals including: 6-boundary of the Central Uralian uplift and Eastern Uralian Plateau; 7-Late Paleozoic and Early Mesozoic faults; 8- recent depressions; 9 – remnants of Early Mesozoic rift basins; 10- reactivated sutures of the eastern part of the Southern Urals (1-Kopeisk fault zone, 2-Uysk-Brient fault zone, 3- Main Uralian Fault Zone, 4- Shikhan fault zone).

Letters on the scheme mark: EEP –Eastern European platform; UFB – uplift of foredeep basin; BRB – Belaya-river block; WUU – Western Uralian Uplift; UP – Ufimian plateau; CUU – Central Uralian Uplift; TUB – Trans-Uralian block; WSD – Western Siberian depression. Blocks of the Eastern Uralian plateau: MB – Magnitogorsk Block, CHB – Chebarkul Block, ZB – Zingeika Block, PB – Plast Block.

Figure 2. (a) Model of the crustal structure and temperature distribution along the URSEIS profile (modified from [*Kukkonen et al.,* 1997]) used in the strength modeling. Temperature distribution is shown by isotherms. The horizontal axis is numbered according to URSEIS profile. Numbers correspond to different lithologies (explanations are in the text). Vertical arrows at the top of the model mark part of the profile for which stress calculations have been done. Black triangles indicate the location of the strength profiles shown on Figure 3. Roman numerals mark the following blocks: I-Eastern European Platform, II-Urals foredeep; III_1-

Western Uralian block, III_2-Central Uralian block, IV-Magnitogorsk block; V- Zingeika block; VI- Plast block; VII-Trans-Uralian block; VIII-Western Siberian depression.

(b) Distribution of viscosity (in 10^{22} $Pa{\cdot}s$) used for numerical modeling.

Figure 3. Strength of the lithosphere for different blocks of the URSEIS profile. Position of blocks (black triangles) is shown on Figure 2 a.

Figure 4. Components of velocity vectors at the surface and base of the model. Notice offset of the maximum of the vertical component of velocity vector at the top (a) and at the base (b) of the model.

a. 1-average rate of vertical movement during the Neogene-Quaternary according to geomorphologic data; 2-calculated vertical component of velocity vector at the top of the model;

b. Vertical component of velocity at the base of the model;

c. Horizontal component of velocity at the base of the model.

Figure 5. Distribution of horizontal component of velocity (isolines) and velocity vectors (arrows) relative to the left side of the model. Notice decollement of the upper and lower "rigid" plates in the central part of the profile.

Figure 6. Distribution of (a) the octahedral shear stress and (b) the damage parameter equal to the ratio of the octahedral shear stress to the mean pressure in the crust of the Southern Urals along the URSEIS profile. Absolute values of stress depend on adopted viscosity values. If apparent viscosity of the lithosphere in the both "rigid" layers is equal to 10^{24} $Pa\ s$, then stress in

Figure b is in *MPa*. The Makarovo fault, a distinct 5 km vertical offset of the Moho, which does not disrupt the overlying Riphean sediments, is situated at the point x=390 km [*Diaconescu et al.,* 1998], where both the damage parameter and the general shear stress have maximum values.

Constraints on the Neogene – Quaternary Geodynamics of the Southern Urals

V. Mikhailov, A. Tevelev., R. Berzin, E. Kiseleva, E. Smolyaninova, A. Suleimanov, E. Timoshkina

AGU indexes: 8102, 8107, 8159, 8164.

Table 1. Creep parameters of rocks used for yield strength calculations.

Material	$A_d\ Mpa^{-n} \cdot s^{-1}$	n	$E\ kJ \cdot mol^{-1}$	Reference
Quartzite	$6.7 \cdot 10^{-6}$	*2.4*	*156*	*Ranalli, 1997*
Quartz diorite	$1.3 \cdot 10^{-3}$	*2.4*	*219*	*Kirby and Kronenberg, 1987*
Mafic granulite	$1.4 \cdot 10^{4}$	*4.2*	*445*	*Ranalli, 1997*
Peridotite	$2.5 \cdot 10^{4}$	*3.5*	*532*	*Ranalli, 1997*
Olivine	$4.0 \cdot 10^{6}$	*3.0*	*540*	*Evans and Kohlstedt, 1995*

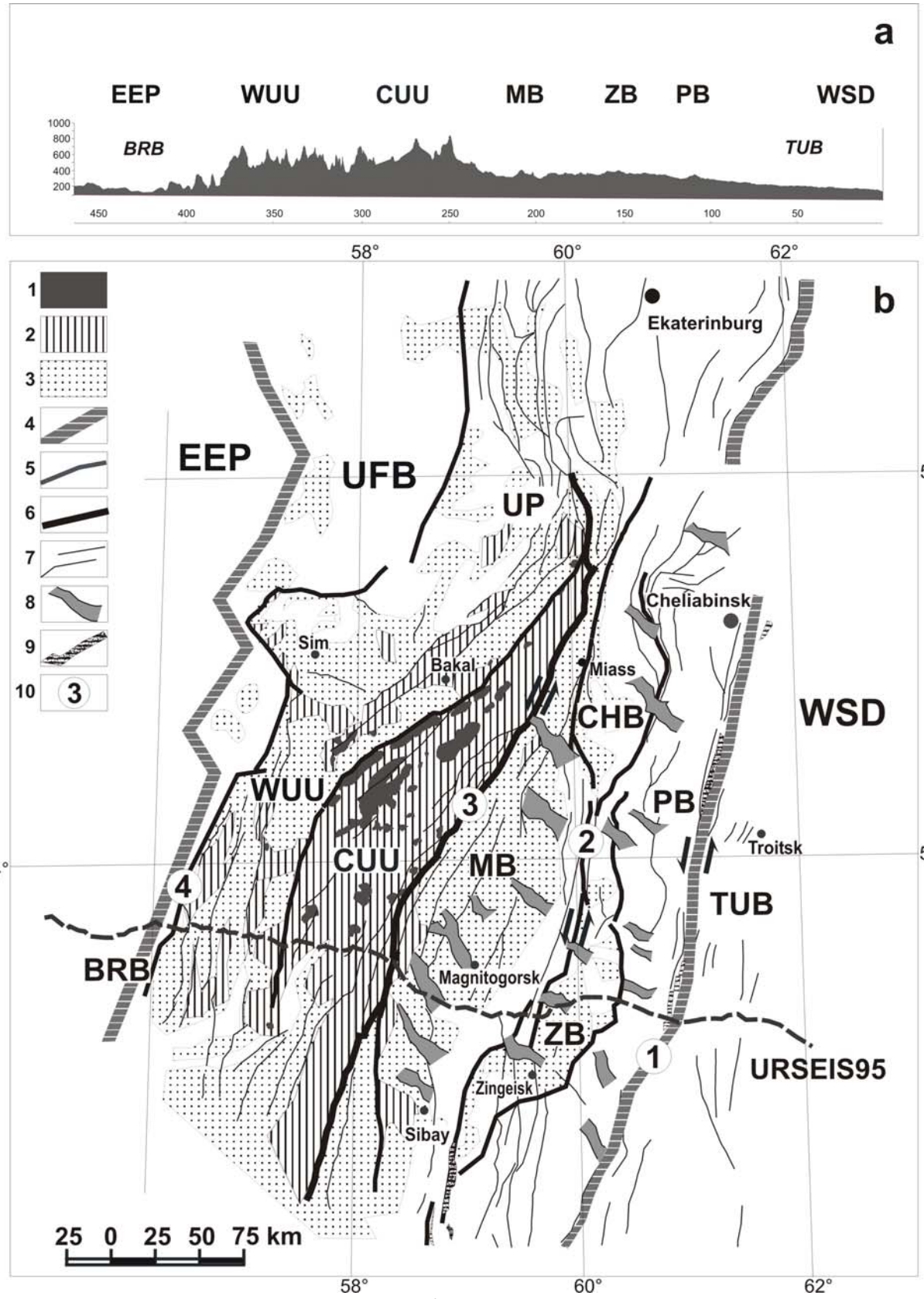
a
EEP
WUU
CUU
MB
ZB
PB
WSD
BRB
TUB
1000
800
600
400
200
450
400
350
300
250
200
150
100
50
b
58°
60°
62°
56°
54°
1
2
3
4
5
6
7
8
9
10
Ekaterinburg
EEP
UFB
UP
Cheliabinsk
Sim
Bakal
Miass
CHB
WSD
WUU
PB
CUU
MB
Troitsk
TUB
BRB
Magnitogorsk
ZB
URSEIS95
Zingeisk
Sibay
25 0 25 50 75 km

Figure 1

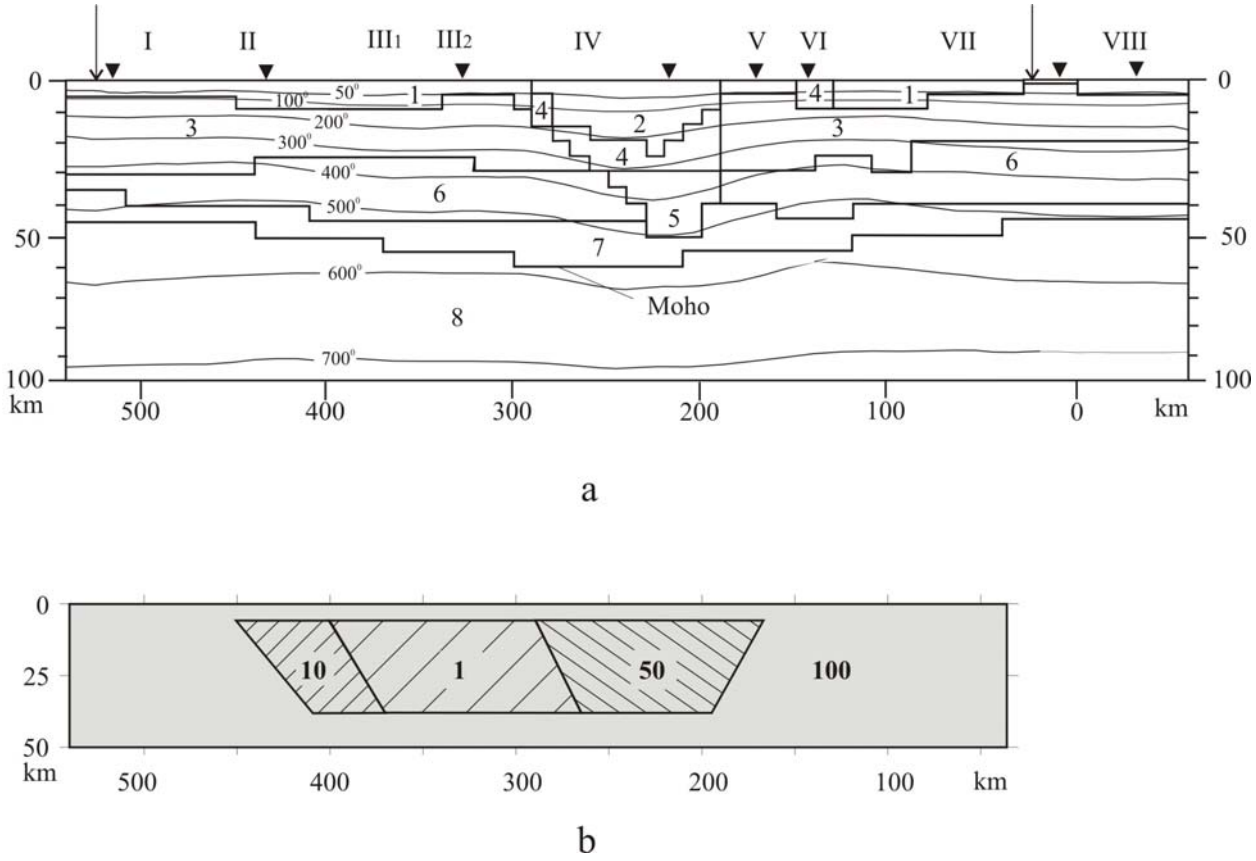
I
II
III1
III2
IV
V
VI
VII
VIII
0
50
100
km
500
400
300
200
100
0
km
50°
100°
200°
300°
400°
500°
600°
700°
Moho
1
2
3
4
5
6
7
8
a
0
25
50
km
500
400
300
200
100
km
10
1
50
100
b

Figure 2

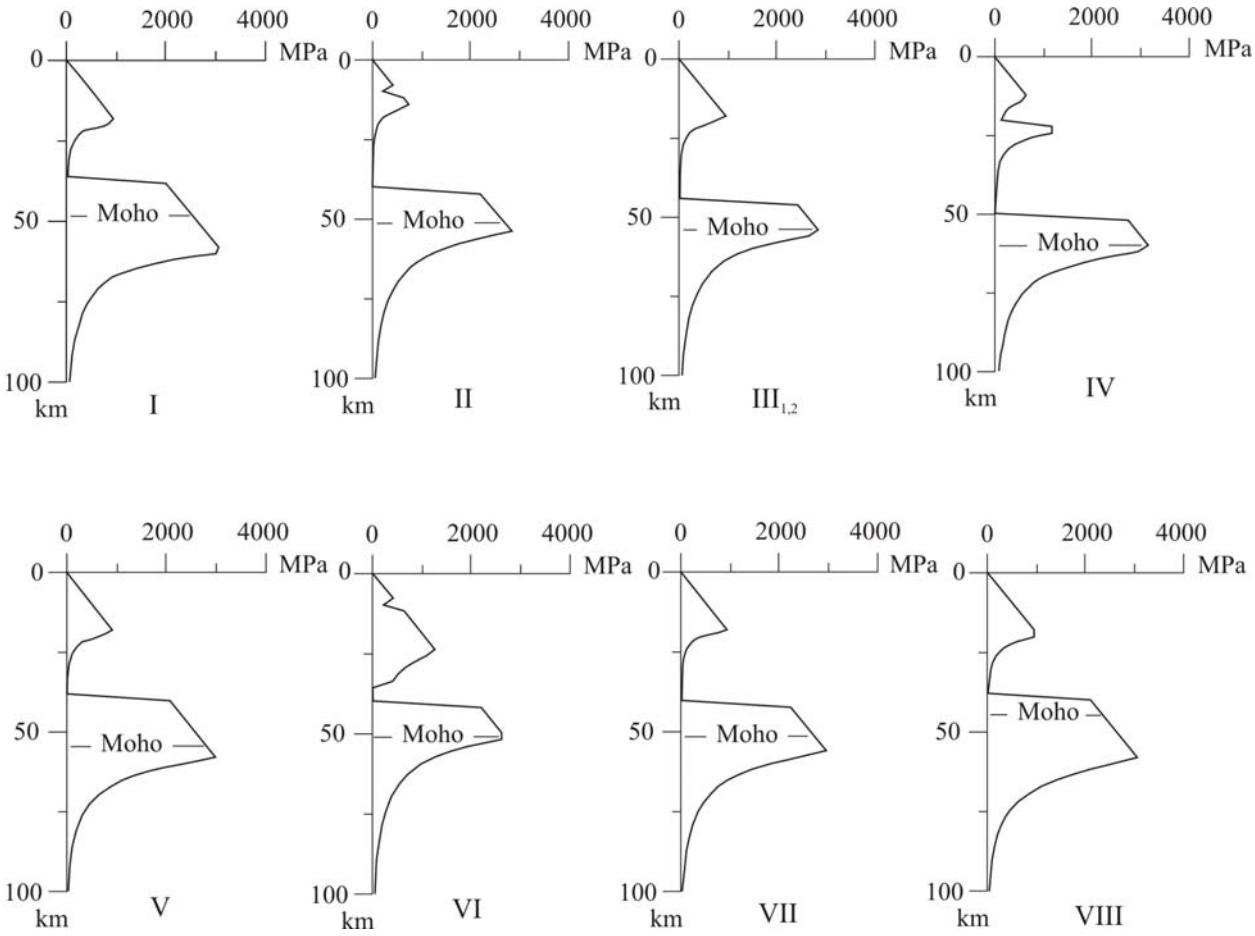

Figure 3

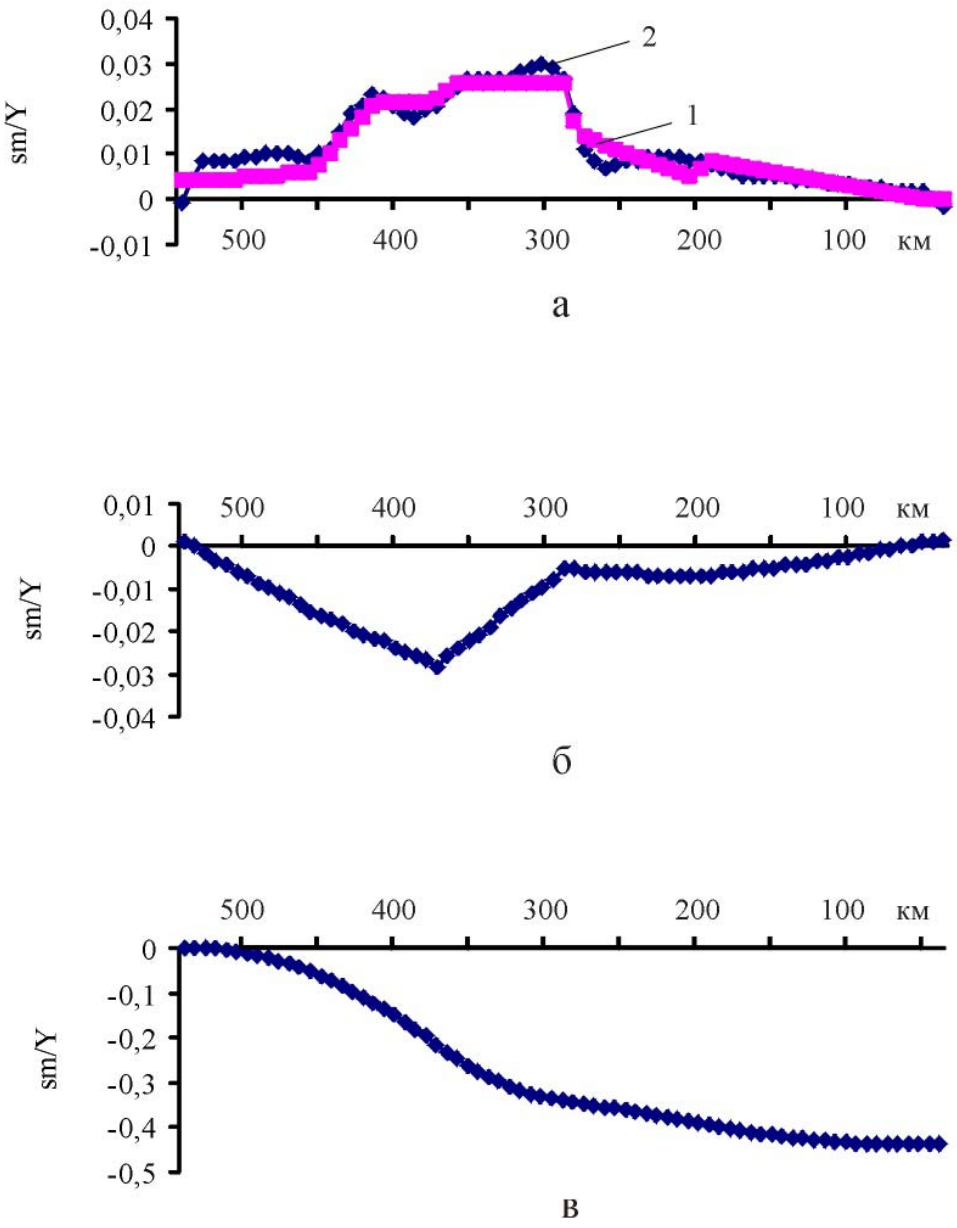
0,04
0,03
0,02
0,01
0
-0,01
sm/Y
500
400
300
200
100
км
2
1
а
0,01
0
-0,01
-0,02
-0,03
-0,04
sm/Y
500
400
300
200
100
км
б
0
-0,1
-0,2
-0,3
-0,4
-0,5
sm/Y
500
400
300
200
100
км
в

Figure 4

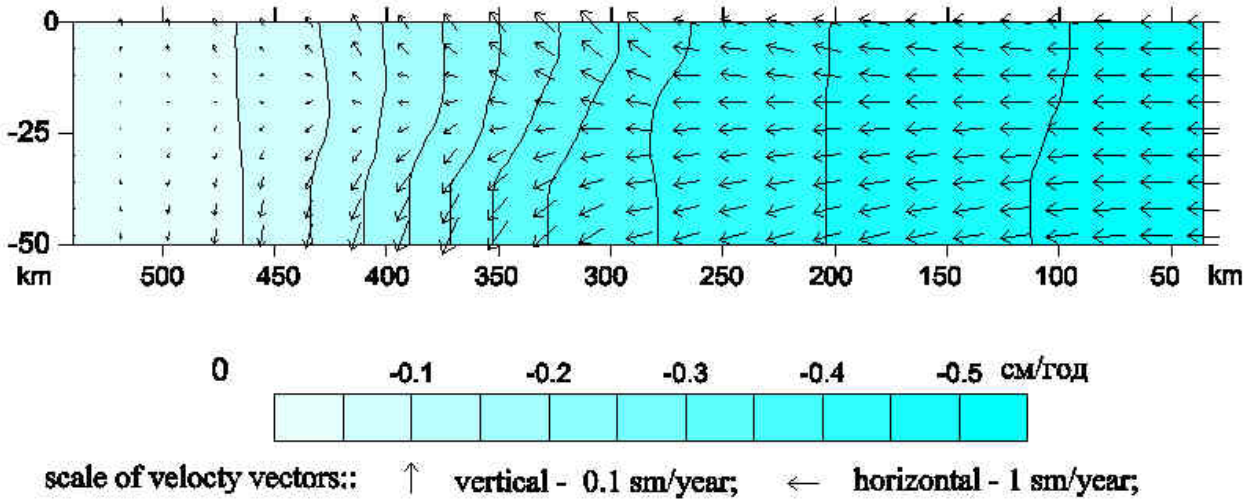

Figure 5

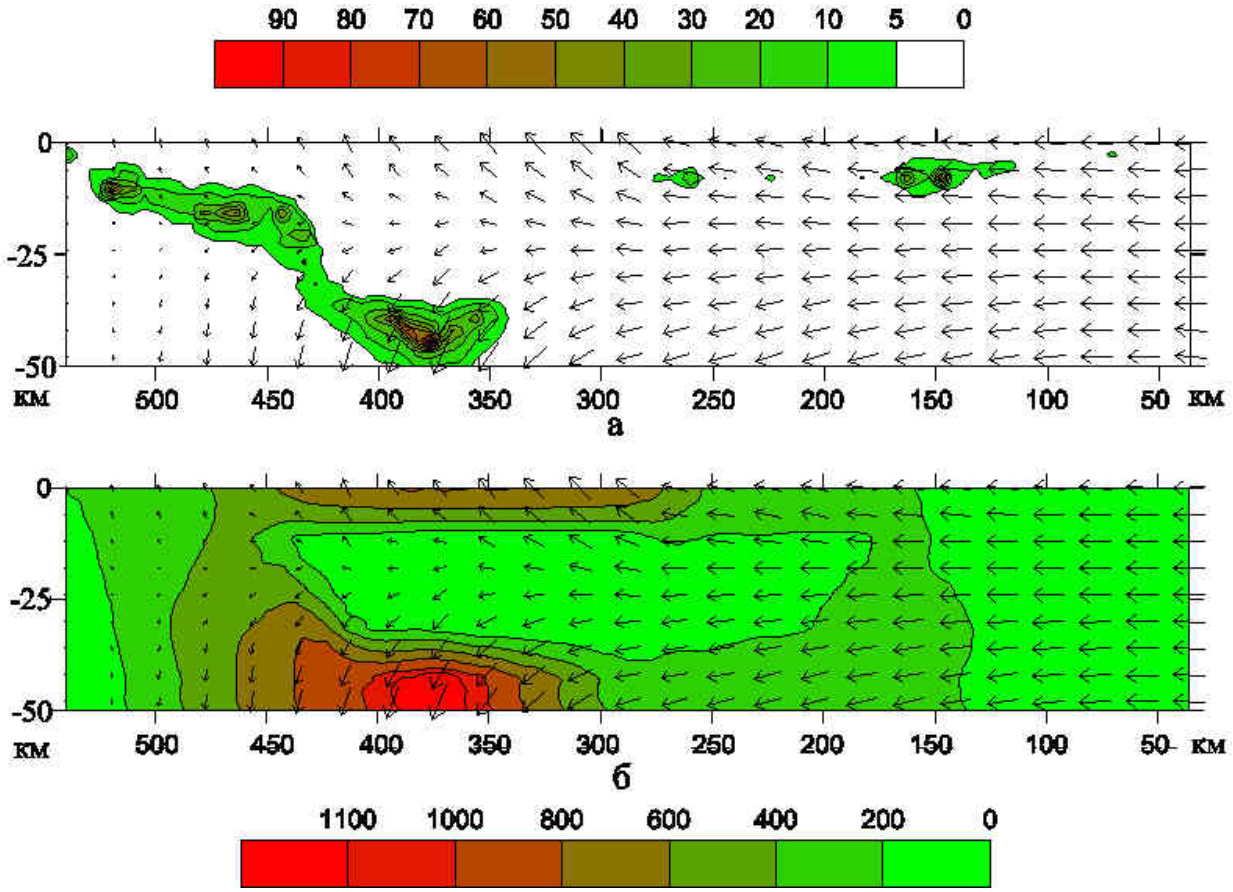

Figure 6